CDF/ANAL/EXOTIC/PUBLIC/9219

Search for Standard Model Higgs Boson Production in Association with $W^{\pm}$ Boson at CDF with 1.9 fb^{-1}

The CDF Collaboration
URL http://www-cdf.fnal.gov
(Dated: February 28, 2008)

We present a search for Standard Model Higgs boson production in association with a $W^{\pm}$ boson. This search uses data corresponding to an integrated luminosity of 1.9 fb^{-1}. We select events matching the W + jets signature using leptons from both the central and forward regions of the detector. We futher require at least one jet to be identified as a b-quark jet. To further increase discrimination between signal and background, we use kinematic information in an artificial neural network. The number of tagged events and the resulting neural network output distributions are consistent with the Standard Model expectations, and we set an upper limit on the WH production cross section times branching ratio $\sigma(p\bar{p} \to W^{\pm}H) \times BR(H \to b\bar{b}) <$ 1.0 to 1.2 pb for Higgs masses from 110 GeV/c^2 to 150 GeV/c^2 at 95% confidence level.

Preliminary Results for Winter 2008 Conferences

I. INTRODUCTION

The success of the Standard Model in explaining and predicting experimental data provides strong motivation for the existence of a neutral Higgs boson. Current electroweak fits combined with direct searches from LEP2 indicate the mass of the Higgs boson is less than $182\,\mathrm{GeV}/c^2$ at 95% confidence level [1, 2].

In proton-antiproton collisions of $\sqrt{s} = 1.96\,\mathrm{TeV}$ at the Tevatron, the Standard Model Higgs boson may be produced in association with a W boson [3]. For low Higgs masses (below $140\,\mathrm{GeV}/c^2$) the dominant decay mode is $H \to b\bar{b}$. The final state from the WH production is therefore $\ell\nu b\bar{b}$, where the high-p_T lepton from the W decay provides an ideal trigger signature.

The previously published WH search from CDF [4] was performed in a dataset with integrated luminosity equivalent to $955\,\mathrm{pb}^{-1}$. This analysis uses about 2 times of the previous data and employs a neural network to improve discrimination between signal and background.

II. DATA SAMPLE & EVENT SELECTION

We use data collected through May 2007, corresponding to an integrated luminosity of $1.9\,\mathrm{fb}^{-1}$. The events are collected by the CDF II detector and classified according to their trigger type.

Central leptons event enter the analysis from high-p_T electron or muon triggers which have an 18 GeV threshold [5]. The electron or muon is further required offline to be isolated with E_T (or p_T) $> 20\,\mathrm{GeV}$. Central lepton events having the W+jets signature are confirmed with a missing transverse energy requirement ($\not\!\!E_T > 20\,\mathrm{GeV}$).

We select forward (plug) electron events with a trigger intended for W candidate events. The plug electron trigger requires both a plug electron candidate and missing transverse energy. Plug electrons events are futher required offline to have $E_T > 20\,\mathrm{GeV}$ and $\not\!\!E_T > 25\,\mathrm{GeV}$. We increase the purity of the sample by applying cuts intended to remove fake events from QCD processes. Our QCD veto consists of the following cuts:

- Linear cut on the $\not\!\!E_T$ and the azimuthal angle (ϕ) between the $\not\!\!E_T$ and the each of the jets ($\not\!\!E_T > 45-(30\cdot|\Delta\phi|)$).
- Large transverse mass of the reconstructed W ($M_T(W) > 20$)
- Large $\not\!\!E_T$ significance $\not\!\!E_T^{sig}$, where $\not\!\!E_T^{sig}$ is defined as ratio of $\not\!\!E_T$ to a weighted sum of factors correlated with mismeasurement, such as angles between the $\not\!\!E_T$ and the jet and amount of jet energy corrections.

The events from both trigger types are classified according to the number of jets having $E_T > 20\,\mathrm{GeV}$ and $|\eta| < 2.0$. Because the Higgs boson decays to $b\bar{b}$ pairs, we employ b-tagging algorithms which relies on the long lifetime and large mass of the b quark.

A. Bottom Quark Tagging Algorithms

To greatly reduce the backgrounds to this Higgs search, we require that at least one jets in the event be identified as containing b-quarks by one of three b-tagging algorithms. The secondary vertex tagging algorithm identifies b quarks by fitting tracks displaced from the primary vertex. This method has been used in other Higgs searches and top analyses [4, 6]. In addition, we add jet probability tagging algorithm that identifies b quarks by requiring a low probability that all tracks contained in a jet originated from the primary vertex, based on the track impact parameters [7]. To be considered for double tag category, an event is required to have either two secondary vertex tags, or one secondary vertex tag and one jet probability tag.

Furthermore we also make use of exactly one b-tagged events with the secondary vertex tagging algorithm. To improve signal-to-background ratio for one tag events, we employ neural network b-tagging algorithm applied in previous analysis [4]. This neural network is tuned for only jets tagged by the secondary vertex tagging algorithm. The purity of b-jets tagged by this algorithm is improved.

B. Total WH Acceptance

The signal acceptance is measured in a sample of Monte Carlo events generated with the PYTHIA program [8]. The detection efficiency for signal events is defined as:

$$\epsilon_{WH\to l\nu b\bar{b}} = \epsilon_{Z0}\cdot\epsilon_{trig}\cdot\epsilon_{leptonid}\cdot\epsilon_{\rm iso}\cdot\epsilon^{MC}_{WH\to\ell\nu b\bar{b}}\cdot\left(\sum_{l'=e,\mu,\tau} Br(W\to\ell\nu)\right), \quad (1)$$

where $\epsilon^{MC}_{WH\to\ell\nu b\bar{b}}$ is the fraction of signal events (with $|z_0| < 60\,\mathrm{cm}$) which pass the kinematic requirements. The effect of the b-tagging scale factor in this fraction is considered by applying scale factor 0.95 ± 0.05. The quantity ϵ_{Z0} is the efficiency of the $|z_0| < 60$cm cut; ϵ_{trig} is the trigger efficiency for high p_T leptons; $\epsilon_{leptonid}$, is the efficiency to identify a lepton; ϵ_{iso} is efficiency of the energy isolation cut ; and $Br(W\to\ell\nu)$ is the branching ratio for leptonic W decay. For plug electrons, ϵ_{trig} is parameterized as a function of the trigger missing transverse energy ($\not\!\!E_T^{raw}$) and the E_T of the electron.

Fig. 1 shows the overall acceptance for the single-tag and the double-tag categories–including all systematic effects–as a function of Higgs mass. The acceptance for the double secondary vertex tagged category increases from (0.42±0.04)% for a Higgs mass of $110\,\mathrm{GeV}/c^2$ to (0.51±0.05)% for a Higgs mass of $150\,\mathrm{GeV}/c^2$. The acceptance of the secondary vertex plus jet probability category ranges from (0.36±0.04)% to (0.43±0.05)% over the same mass range. The acceptance of one neural network tagged category ranges from (0.91±0.05)% to (1.01±0.06)% over the same mass range.

These two categories of double-tagged events and one category of one neural network tagged events are defined exclusively, so the total acceptance is given by the sum of the acceptance for the three categories.

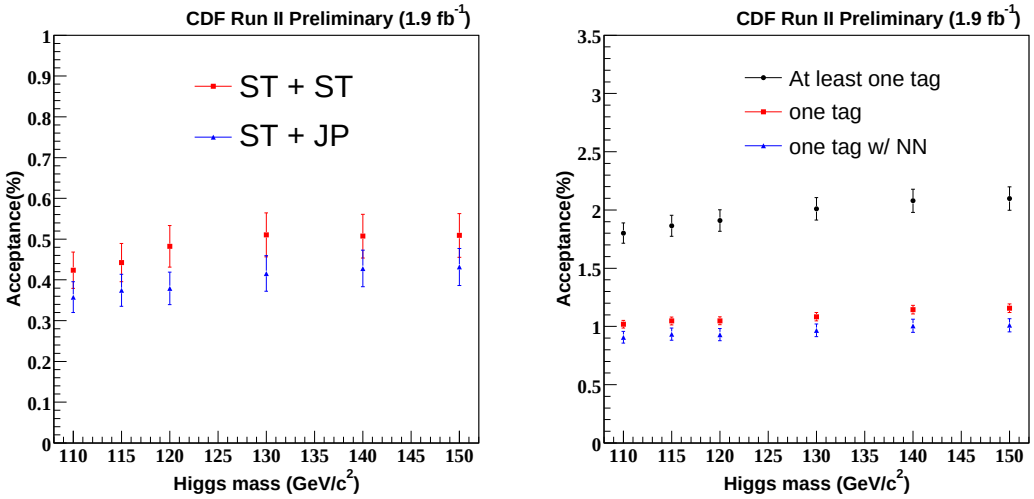

FIG. 1: Calculated WH acceptance for the double b-tagging selection criteria (left). "Double tag" refers to the double secondary vertex tag category while "ST + JP" refers to the secondary vertex plus jet probability category. Calculated WH acceptance for the one b-tagging selection criteria (right). "One tag w/ NN" referees to one neural network tag category. For the reference, the acceptance for at least one secondary vertex tagged and exactly one secondary vertex tagged category without neural network tag. These three categories are defined exclusively, so the total acceptance is just the sum of the acceptance for the three categories.

III. BACKGROUNDS

This analysis builds on the method of background estimation detailed in Ref. [6]. In particular, the contributions from the following individual backgrounds are calculated: falsely b-tagged events, W production with heavy flavor quark pairs, QCD events with false W signatures, top quark pair production, and electroweak production (diboson, single top).

Njet	2jet	3jet	>=4jet
Pretag Events	32242	5496	1494
Mistag	3.88±0.35	2.41±0.24	1.62± 0.14
$Wb\bar{b}$	37.93±16.92	14.05±5.49	7.39± 2.93
$Wc\bar{c}$	2.88±1.25	1.52±0.61	1.15± 0.47
$t\bar{t}$(6.7pb)	19.05±2.92	54.67±8.38	94.93± 14.56
Single top(s-ch)	6.90±1.00	2.28±0.33	0.61± 0.09
Single top(t-ch)	1.60±0.23	1.43±0.21	0.50± 0.07
WW	0.17±0.02	0.15±0.02	0.16± 0.02
WZ	2.41±0.26	0.68±0.07	0.16± 0.02
ZZ	0.06±0.01	0.06±0.01	0.02±0.001
$Z->\tau\tau$	0.25±0.04	0.19±0.03	0.06±0.01
nonW QCD	5.50±1.00	2.56±0.48	1.02± 0.22
Total Bkg	80.62±18.75	79.99±10.92	107.63± 15.15
WH signal (120 GeV)	0.94±0.11	Control region	Control region
Observed Events	83	88	118

TABLE I: Background summary table for central leptons double secondary vertex tag category.

We estimate the number of falsely b-tagged events (mistags) by counting the number of negatively-tagged events, that is, events in which the measured displacement of the secondary vertex is opposite the b jet direction. Such negative tags are due to tracking resolution limitations, but they provide a reasonable estimate of the number of false positive tags after a correction for material interactions and long-lived light flavor particles.

The number of events from W + heavy flavor is calculated using information from both data and Monte Carlo programs. We calculate the fraction of W events with associated heavy flavor production in the ALPGEN Monte Carlo program interfaced with the PYTHIA parton shower code [8, 9]. This fraction and the tagging efficiency for such events are applied to the number of events in the original W+jets sample after correcting for the $t\bar{t}$ and electroweak contributions.

For central leptons we constrain the number of QCD events with false W signatures by assuming the lepton isolation is independent of $\not\!\!E_T$ and measuring the ratio of isolated to non-isolated leptons in a $\not\!\!E_T$ sideband region. The result in the tagged sample can be calculated in two ways: by applying the method directly to the tagged sample, or by estimating the number of non-W QCD events in the pretag sample and applying an average b-tagging rate.

For plug electrons we use the $\not\!\!E_T$ shape difference between the non-w and the other background models to constrain the amount of QCD events. We perform a likelihood fit to the $\not\!\!E_T$ distribution to determine the total amount of QCD. We deduce the QCD fraction in the signal region by integrating the fitted distributions above our $\not\!\!E_T$ cut (25 GeV). The non-W contribution to the tagged sample can estimated by the same methods as the central leptons.

The summary of the background contributions to the central lepton selection are shows in Tables I to III. The double secondary vertex tagged selection is given in Table I, the summary in the case of secondary vertex plus jet probability tagged events is shown in Table II, and the summary in the case of one neural network tagged events is shown in Table III. Tables IV through VI show the background expecations for the plug electrons.

Because the expected number of Higgs signal events is small in the 1-,3-, and 4-jet bins, the reasonable agreement between predicted backgrounds and observed data in Fig. 2 gives us confidence in our overall background estimate.

IV. SYSTEMATIC UNCERTAINTIES

The uncertainties on the signal acceptance currently have the largest effect on the Higgs sensitivity. The b-tagging uncertainty is dominated by the uncertainty on the data/MC scale factor $S = 0.95 \pm 0.04$ (stat.+ sys.). The uncertainties due to initial state radiation and final state radiation are estimated by changing the parameters related to ISR and FSR, halving and doubling the default values. The difference from the nominal acceptance is taken as the systematic uncertainty. Other uncertainties on parton distribution functions, trigger efficiencies, or lepton identification contribute to a smaller extent to the overall uncertainty. The summary of these systematic uncertainties on the signal acceptance is given in Table VII.

Njet	2jet	3jet	>=4jet
Pretag Events	32242	5496	1494
Mistag	11.73±0.92	8.11±0.64	8.39±0.58
$Wb\bar{b}$	31.15±14.03	11.47±4.55	6.55±2.63
$Wc\bar{c}$	7.87±3.43	4.38±1.76	3.09±1.27
$t\bar{t}$(6.7pb)	15.56±2.39	47.48±7.28	79.81±12.24
Single top(s-ch)	5.14±0.75	1.90±0.27	0.53±0.07
Single top(t-ch)	1.87±0.27	1.49±0.22	0.44±0.06
WW	0.93±0.11	0.63±0.08	0.47±0.06
WZ	1.84±0.20	0.59±0.06	0.19±0.02
ZZ	0.08±0.01	0.04±0.003	0.02±0.002
$Z->\tau\tau$	1.29±0.20	0.53±0.08	0.20±0.03
nonW QCD	9.55±1.73	4.87±0.93	1.80±0.40
Total Bkg	86.99±17.99	81.46±10.22	101.49±13.08
WH signal (120 GeV)	0.74±0.09	Control region	Control region
Observed Events	90	80	106

TABLE II: Background summary table for central leptons secondary vertex plus jet probability tag category.

Njet	1jet	2jet	3jet	>=4jet
Pretag Events	196160	32242	5496	1494
Mistag	236.7±19.36	107.1±9.38	41.84±3.84	20.97±1.91
$Wb\bar{b}$	431.7±182.4	215.6±92.34	61.78±24.68	26.14±10.43
$Wc\bar{c}$	514.4±154.7	167.0±62.14	45.40±15.31	17.71±6.86
$t\bar{t}$(6.7pb)	11.85±1.82	60.68±9.30	111.0±17.03	122.4±18.76
Single top(s-ch)	7.09±1.03	14.38±2.09	3.91±0.57	0.97±0.14
Single top(t-ch)	23.31±3.41	29.57±4.33	6.24±0.91	1.11±0.16
WW	7.21±0.89	15.45±1.91	4.61±0.57	1.03±0.13
WZ	5.52±0.59	7.59±0.81	1.76±0.19	0.48±0.05
ZZ	0.17±0.02	0.31±0.03	0.14±0.01	0.07±0.01
$Z->\tau\tau$	14.58±2.25	7.27±1.12	2.39±0.37	0.71±0.11
nonW QCD	465±83.21	184.7±33.04	44.83±8.57	17.03±3.67
Total Bkg	1717.6±347.9	809.61±159.38	323.92±45.5	208.57±26.24
WH signal (120 GeV)	Control region	1.82±0.15	Control region	Control region
Observed Events	1812	805	306	215

TABLE III: Background summary table for central leptons with one secondary vertex tag with NN tag category.

Njet	2jet	3jet	>=4jet
Pretag Events	5879	1010	202
Mistag	1.00±0.18	0.46±0.06	0.35±0.15
$Wb\bar{b}$	7.40±3.96	2.34±1.15	0.47±0.26
$Wc\bar{c}$	0.96±0.49	0.33±0.37	0.07± 0.03
$t\bar{t}$(6.7pb)	2.14±0.34	5.69±0.89	9.11± 1.43
Single top(s-ch)	0.69±0.10	0.22±0.03	0.06± 0.01
Single top(t-ch)	0.22±0.04	0.18±0.03	0.06± 0.01
WW	0.01±0.01	0.03±0.02	0.02± 0.01
WZ	0.58±0.06	0.12±0.02	0.04± 0.01
ZZ	0.00±0.00	0.00±0.00	0.00±0.00
$Z->\tau\tau$	0.00±0.00	0.00±0.00	0.00±0.00
nonW QCD	1.16±0.44	0.96±0.50	0.51±0.44
Total Bkg	14.18±4.03	10.32±1.58	10.67± 1.52
WH signal (120 GeV)	0.09±0.01	Control region	Control region
Observed Events	11	12	11

TABLE IV: Background summary table for plug electron events with two secondary vertex tags.

Njet	2jet	3jet	>=4jet
Pretag Events	5879	1010	202
Mistag	3.18±0.49	1.71±0.33	0.74± 0.29
$Wb\bar{b}$	6.23±3.37	2.00±0.99	0.45±0.24
$Wc\bar{c}$	1.53±0.81	0.76±0.38	0.21± 0.11
$t\bar{t}$(6.7pb)	1.79±0.31	4.72±0.80	7.03± 1.19
Single top(s-ch)	0.51±0.08	0.16±0.03	0.04± 0.01
Single top(t-ch)	0.24±0.04	0.16±0.03	0.05± 0.01
WW	0.12±0.03	0.10±0.03	0.07± 0.02
WZ	0.42±0.05	0.13±0.02	0.03± 0.01
ZZ	0.01±0.00	0.00±0.00	0.00±0.00
$Z->\tau\tau$	0.01±0.00	0.01±0.00	0.01±0.00
nonW QCD	1.51±0.55	1.78±0.88	0.79±0.67
Total Bkg	15.54±3.56	11.53±1.63	9.43± 1.42
WH signal (120 GeV)	0.06±0.01	Control region	Control region
Observed Events	12	10	10

TABLE V: Background summary table for plug electron events with one secondary vertex tag + Jet Probability tag

Njet	1jet	2jet	3jet	>=4jet
Pretag Events	39942	5879	1010	202
Mistag	91.19±8.32	28.47±3.30	6.48±1.20	0.78±0.60
$Wb\bar{b}$	98.10±50.81	43.09±12.33	10.74±3.10	1.79±0.62
$Wc\bar{c}$	116.9±49.6	33.37±9.55	7.90±2.28	1.21±0.42
$t\bar{t}$(6.7pb)	1.36±0.20	7.17±1.00	12.30±1.71	13.89±1.93
Single top(s-ch)	0.96±0.13	1.53±0.20	0.41±0.05	0.09±0.01
Single top(t-ch)	3.88±0.51	3.54±0.47	0.73±0.10	0.12±0.02
WW	1.23±0.12	3.00±0.20	0.74±0.09	0.14±0.04
WZ	1.38±0.08	1.62±0.09	0.43±0.04	0.08±0.02
ZZ	0.01±0.00	0.02±0.00	0.01±0.00	0.00±0.00
$Z->\tau\tau$	0.43±0.05	0.24±0.03	0.11±0.01	0.03±0.00
nonW QCD	18.76±6.98	18.34±5.54	5.54±2.59	3.18±2.53
Total Bkg	334.2±71.8	140.4±16.9	45.39±5.09	21.31±3.33
WH signal (120 GeV)	Control region	0.20±0.01	Control region	Control region
Observed Events	299	136	48	25

TABLE VI: Background summary table for plug electron events with one secondary vertex tag with a NN tag.

V. ARTIFICIAL NEURAL NETWORK

To further improve signal to background separation we employ an artificial neural network. This neural network combines six kinematic variables into a single function with better discrimination between the Higgs signal and the background processes than any of the variables individually. To train the neural network, JETNET package [10]. The input variables are defined below:

Dijet invariant mass+: The invariant mass reconstructed from the two jets. If there are additional looser jets, the loose jet that is closest to one of the two jets is included in this invariant mass calculation.

Total System p_T: The vector sum of the transverse momenta of the lepton, the $\not\!\!E_T$, and the two jets.

p_T **Imbalance:** The scalar sum of the lepton and jet transverse momenta minus the $\not\!\!E_T$.

$\sum E_T$ **(loose jets):** The scalar sum of the loose jet transverse energy.

$M_{l\nu j}^{min}$**:** The invariant mass of the lepton, $\not\!\!E_T$and one of the two jets, where the jet is chosen to give the minimum invariant mass. The p_z of neutrino is ignored for this quantity.

ΔR **(lepton-ν):** The distance between the direction of lepton and neutrino in $\eta-\phi$ plane, where the p_z of the neutrino is taken from largest $|p_z|$ calculated from W mass constraint.

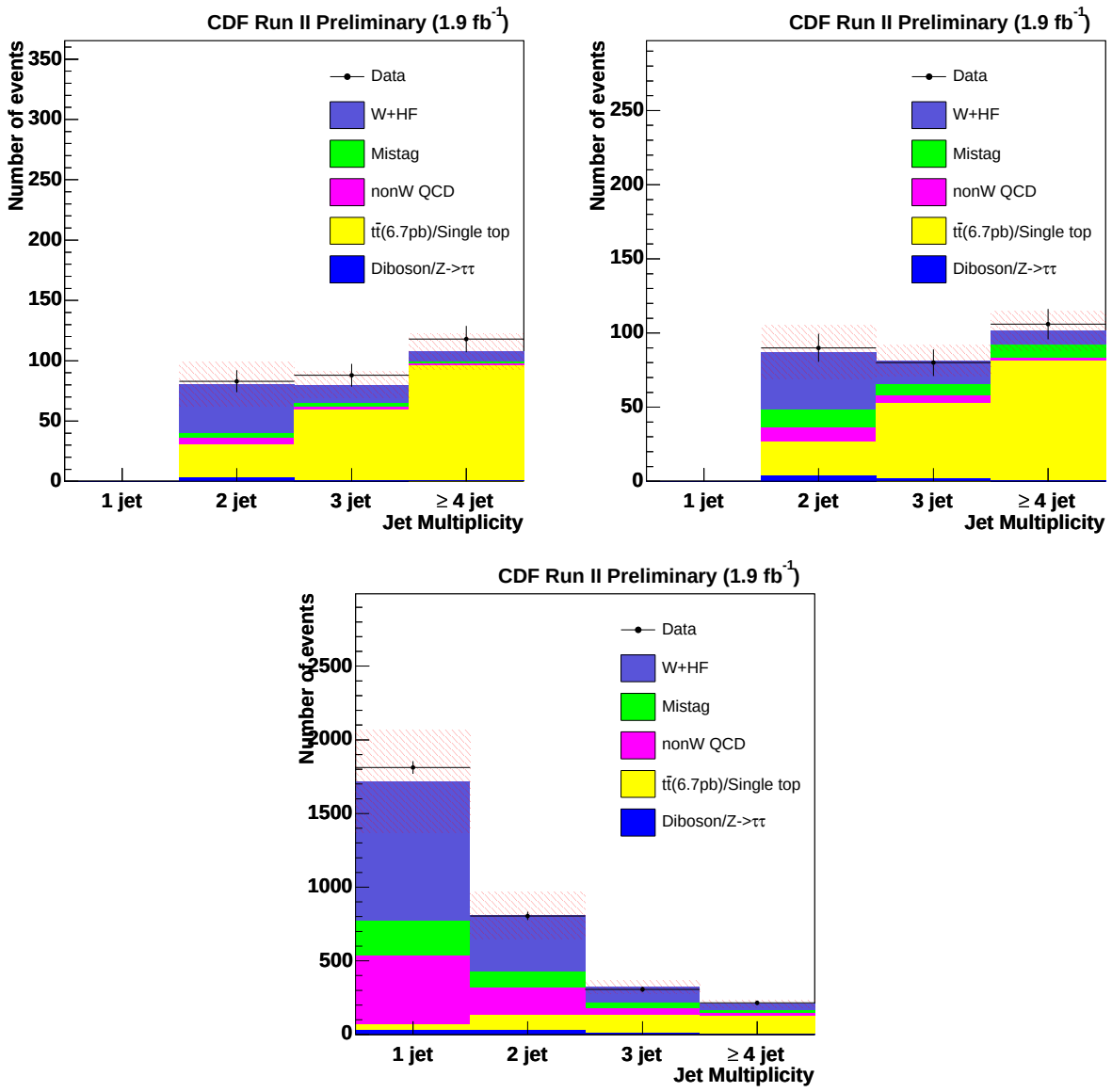

FIG. 2: Predicted and observed W+jet multiplicity with all background contributions for central lepton events. Results are shown for three disjoint selections: double secondary vertex tagged (top left), secondary vertex plus jet probability (top right) and one neural network tag (bottom).

The training is defined such that the neural network attempts to produce an output as close to 1.0 as possible for Higgs signal events and as close to 0.0 as possible for background events. For optimal sensitivity, a different neural network is trained for each Higgs mass considered.

VI. RESULTS

We perform a direct search for an excess in the signal region of the neural network output distribution from single-tagged and double-tagged W+2 jet events. A binned maximum likelihood technique is used to estimate upper limits on Higgs production by constraining the number of background events to the estimates within uncertainties. For optimal sensitivity, the search is performed simultaneously in the separate double secondary vertex tagged, the secondary vertex plus jet probability tagged samples and one neural network tagged samples. We perform separate searches for plug electrons and central leptons. Ultimately, our most sensitive search looks looks at both lepton types

Source	Uncertainty (%)		
	ST+ST	ST+JP	one tag w/ NN tag
Lepton ID	∼2%	∼2%	∼2%
Trigger	<1%	<1%	<1%
ISR/FSR	5.2%	4.0%	2.9%
PDF	2.1%	1.5%	2.3%
JES	2.5%	2.8%	1.2%
b-tagging	8.4%	9.1%	3.5%
Total	10.6%	10.5%	5.6%

TABLE VII: Systematic uncertainty on the WH acceptance. "ST+ST" refers to double secondary vertex tagged events while "ST+JP" refers to secondary vertex plus jet probability tagged events. Effects of limited Monte Carlo statistics are included in these values.

simultaneously. The central lepton sensitivity in the three b-tagged categories separately and the combined samples is shown in Fig. 3. The plug electron expected and observed sensitivity for simultaneously fitting the three b-tagged categories is shown in Figure 11.

For central lepton double secondary vertex tagged events, Fig. 4 shows the output distribution for the neural network trained for a Higgs mass of $120\,\mathrm{GeV}/c^2$ in the data compared to the expectations from background. For reference the dijet invariant mass distribution is also shown. Fig. 5 and Fig. 6 shows the same distribution for the secondary vertex plus jet probability tagged events and one neural network tagged events, respectively. The agreement is reasonable, considering the uncertainties in the background distributions. We set an upper limit on the production cross section times branching ratio as a function of m_H, plotted in Fig. 7. The results are also collected in Table VIII.

Figures 8 through 10 show the neural network output distributions for plug electron events in each b-tagging category. The agreement of the neural network output distributions is reasonable in each tag categoy. The large uncertainties on the data points are due to small number of observed events. We set an upper limit on the cross section times branching ratio as a function of m_H as shown in Figure 11. The results shown in the plot are detailed in Table IX.

Finally, we combine our searches across lepton types and b-tagging categories to obtain our best limit. Figure 12 shows the upper limit on the cross secetion times branching ratio as a function of m_H. The results are also detailed in Table X. Figure 12 includes the expected an observed limits for the distinct lepton categories as a reference. As a cross-check, we obtained limits consistent with those shown in Figure 12 using the analysis techniques developed in the CDF single-top searches. Adding the plug electrons yeilds a 2-6% increase in sensitivity over the central leptons.

Higgs Mass	Upper Limit (pb)	
GeV/c^2	Observed	Expected
110	1.4 (8.5)	1.2 (7.6)
115	1.3 (9.7)	1.2 (8.9)
120	1.1 (10.5)	1.0 (10.0)
130	1.1 (17.2)	0.9 (14.0)
140	1.0 (31.9)	0.8 (25.3)
150	0.9 (78.9)	0.7 (61.8)

TABLE VIII: Observed 95% C.L. upper limit on $\sigma(p\bar{p} \to WH) \times BR(H \to b\bar{b})$ for central leptons. The number in parenthesis gives the ratio of the upper limit to the SM expectation.

VII. CONCLUSIONS

We have searched in a $1.9\,\mathrm{fb}^{-1}$ data set for evidence of Standard Model Higgs boson production associated with a W boson. We do not observe any such production in the $H \to b\bar{b}$ mode, and we set upper limits on the production rate times branching ratio. Total rates larger than 1.1 pb are excluded at 95% confidence level for the $115\,\mathrm{GeV}/c^2$ Higgs mass hypothesis, with limits ranging from 1.0 to 1.2 pb for other mass values. These limits represent an improvement by a factor of approximately 2.2 over the previous limits obtained using the $955\,\mathrm{pb}^{-1}$ data set. The improvement expected only from the increase in luminosity is a factor of 1.4, with the additional 60% coming from improvements in b-tagging, event selection, and background modeling, as well as the addition of a neural network discriminant and

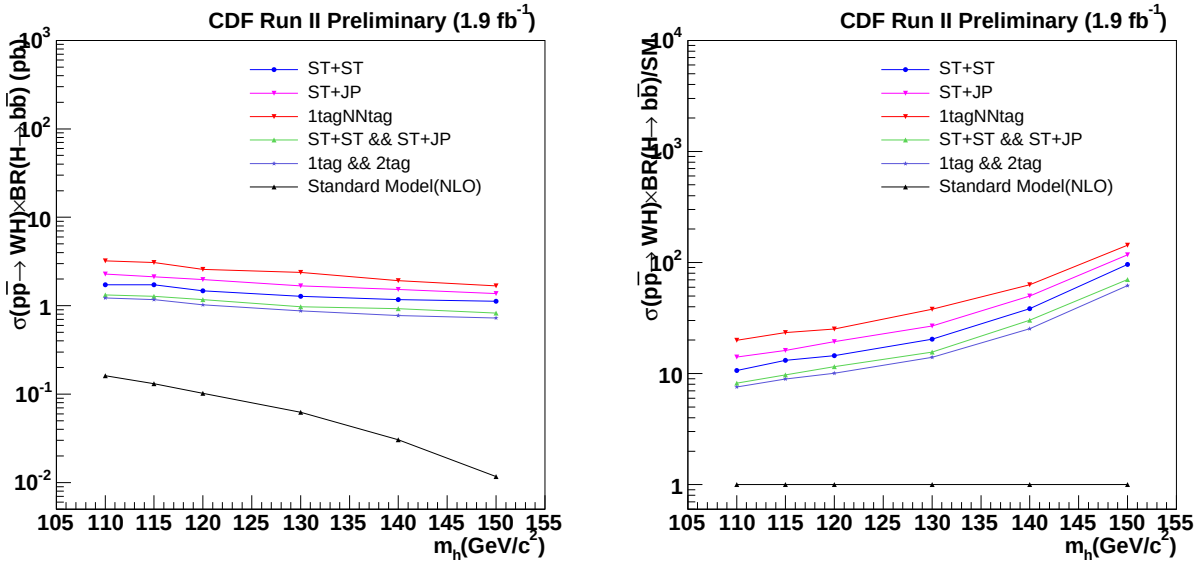

FIG. 3: Expected limits on Higgs production and decay for the separate single-tagged and double-tagged categories and for all categories combined, as a function of the Higgs mass hypothesis. The double secondary vertex tagged category is referred to as "ST+ST", the secondary vertex plus jet probability category is called "ST+JP". While one neural network tagged category is labeled to as "1tagNNtag". The final results combine the two double-tagged categories and one neural network tag category. The plot on the left shows the expected limit in picobarns. The plot on the right shows the expected limit divided by the SM prediction for Higgs cross section.

Higgs Mass	Upper Limit (pb)	
GeV/c^2	Observed	Expected
110 GeV	3.8 (22.8)	5.3 (31.6)
115 GeV	3.5 (25.8)	4.8 (35.7)
120 GeV	5.1 (47.2)	4.7 (43.7)
130 GeV	4.7 (75.2)	4.3 (68.9)
140 GeV	7.8 (250.2)	3.9 (127.3)
150 GeV	3.4 (282.8)	3.1 (254.6)

TABLE IX: Observed 95% C.L. upper limit on $\sigma(p\bar{p} \to WH) \times BR(H \to b\bar{b})$ for plug electrons. The numbers in parenthesis are ratios to the Standard Model values.

plug electron events. Despite these improvements, the result is still limited by the small number of expected Higgs events given the size of the data set and the selection efficiency.

Acknowledgments

We thank the Fermilab staff and the technical staffs of the participating institutions for their vital contributions. This work was supported by the U.S. Department of Energy and National Science Foundation; the Italian Istituto Nazionale di Fisica Nucleare; the Ministry of Education, Culture, Sports, Science and Technology of Japan; the Natural Sciences and Engineering Research Council of Canada; the National Science Council of the Republic of China; the Swiss National Science Foundation; the A.P. Sloan Foundation; the Bundesministerium für Bildung und Forschung, Germany; the Korean Science and Engineering Foundation and the Korean Research Foundation; the Particle Physics and Astronomy Research Council and the Royal Society, UK; the Russian Foundation for Basic Research; the Comision Interministerial de Ciencia y Tecnologia, Spain; and in part by the European Community's

Higgs Mass	Upper Limit (pb)	
GeV/c^2	Observed	Expected
110 GeV	1.1 (6.8)	1.1 (6.5)
115 GeV	1.1 (8.2)	1.0 (7.3)
120 GeV	1.1 (9.8)	1.0 (8.9)
130 GeV	1.0 (15.8)	1.0 (12.6)
140 GeV	1.2 (37.8)	0.7 (23.4)
150 GeV	1.0 (85.2)	0.7 (57.6)

TABLE X: Observed 95% C.L. upper limit on $\sigma(p\bar{p} \to WH) \times BR(H \to b\bar{b})$ for the combination of central and plug leptons. The numbers shown are ratios to the Standard Model values.

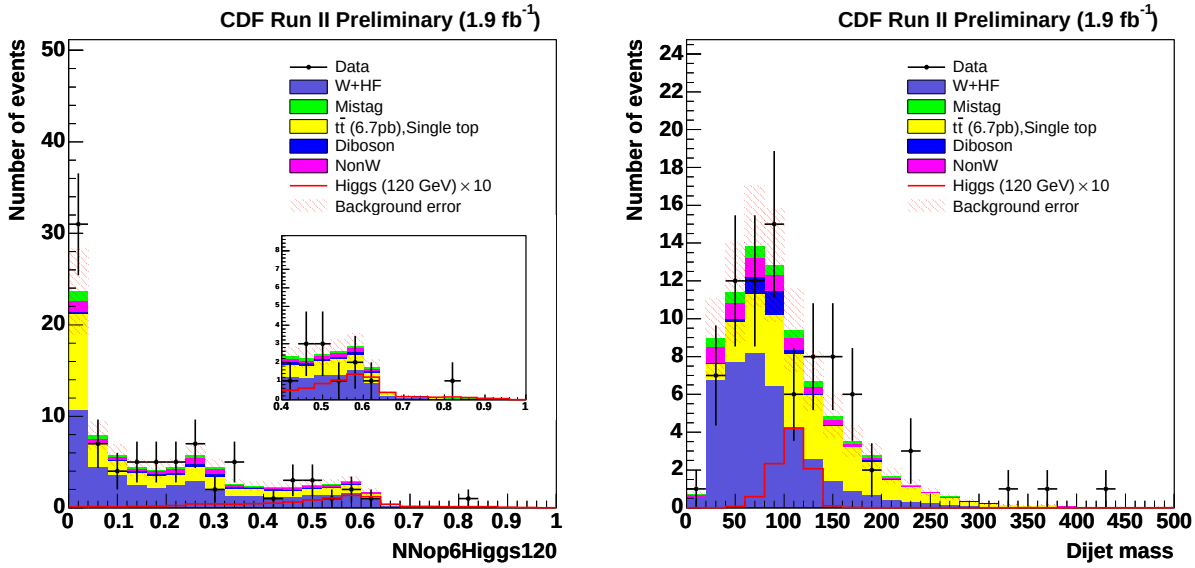

FIG. 4: Predicted and observed output for the neural network trained with a Higgs mass of 120 GeV/c^2 for double secondary vertex tagged events. The output for neural networks trained for other Higgs masses looks similar. For comparison, the dijet mass distribution is also shown.

Human Potential Programme under contract HPRN-CT-20002, Probe for New Physics.

[1] LEP Electroweak Working Group, `http://lepewwg.web.cern.ch/LEPEWWG/`
[2] ALEPH, DELPHI, L3, OPAL. The LEP Working Group for Higgs Boson Searches, Phys. Lett **B565** 61 (2003).
[3] T. Han and S. Willenbrock, Phys. Lett. **B273** (1991) 167;
A. Djouadi, J. Kalinowski, and M. Spira, Comp. Phys. Commun. **108 C** (1998) 56.
[4] T. Aaltonen *et al.*, Phys. Rev. Lett. **100** 041801 (2008).
[5] F. Abe, *et al.*, Nucl. Instrum. Methods Phys. Res. A **271**, 387 (1988);
D. Amidei, *et al.*, Nucl. Instum. Methods Phys. Res. A **350**, 73 (1994);
F. Abe, *et al.*, Phys. Rev. D **52**, 4784 (1995);
P. Azzi, *et al.*, Nucl. Instrum. Methods Phys. Res. A **360**, 137 (1995);
The CDF II Detector Technical Design Report, Fermilab-Pub-96/390-E.
[6] A. Abulencia *et al.*, Phys. Rev. **D71**, 072005 (2005).
[7] D. Buskulic, *et al.* (ALEPH Collaboration), Phys. Lett. B **313**, 535 (1993);
F. Abe *et al.* (CDF Collaboration), Phys. Rev. D **53**, 1051 (1996);
A. Affolder *et al.* (CDF Collaboration), Phys. Rev. D **64**, 032002 (2001), Erratum-ibid: Phys. Rev. D **67**, 119901 (2003).
[8] P. Edén, C. Friberg, L. Lönnblad, G. Miu, S. Mrenna, E. Norrbin, and T. Sjöstrand, Computer Phys. Commun. **135** (2001) 238.
[9] M.L. Mangano *et al.*, JHEP 0307:001, 2003.

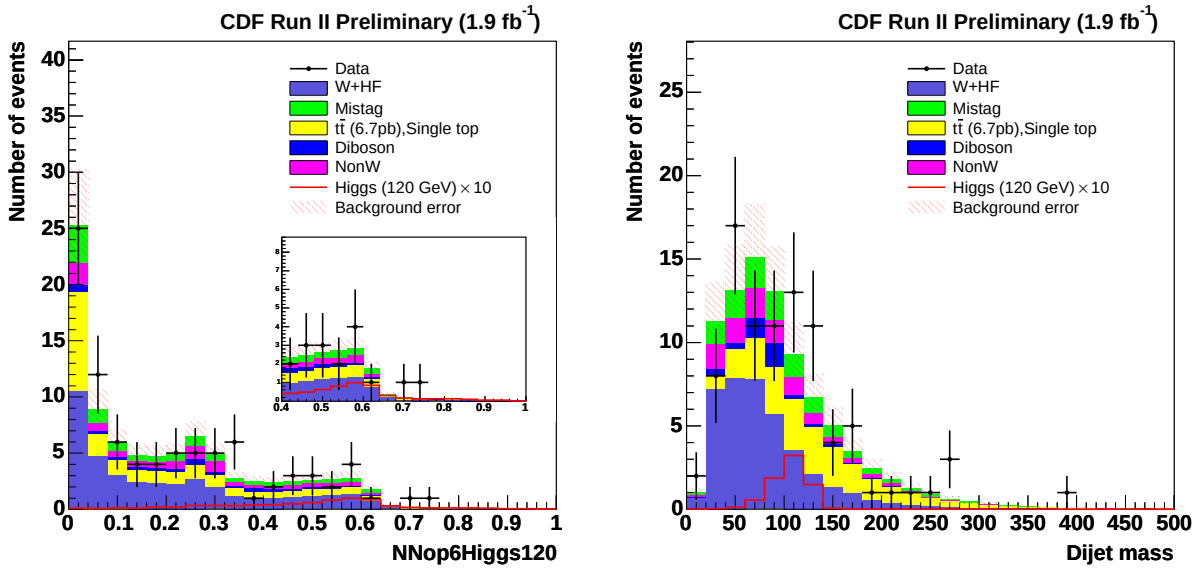

FIG. 5: Predicted and observed output for the neural network trained with a Higgs mass of $120\,\mathrm{GeV}/c^2$ for secondary vertex plus jet probability tagged events. The output for neural networks trained for other Higgs masses looks similar. For comparison, the dijet mass distribution is also shown.

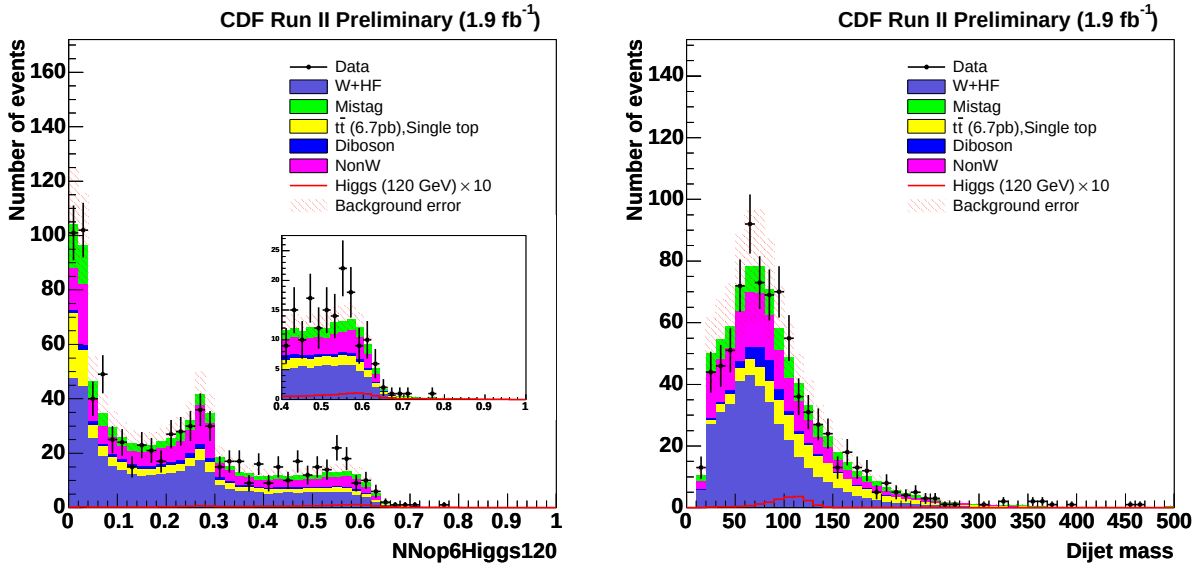

FIG. 6: Predicted and observed output for the neural network trained with a Higgs mass of $120\,\mathrm{GeV}/c^2$ for one neural network tagged events. The output for neural networks trained for other Higgs masses looks similar. For comparison, the dijet mass distribution is also shown.

[10] L. Lönnblad, C. Peterson, and T. Rögnvaldsson, Comp. Phys. Comm. 81 (1994) 185.

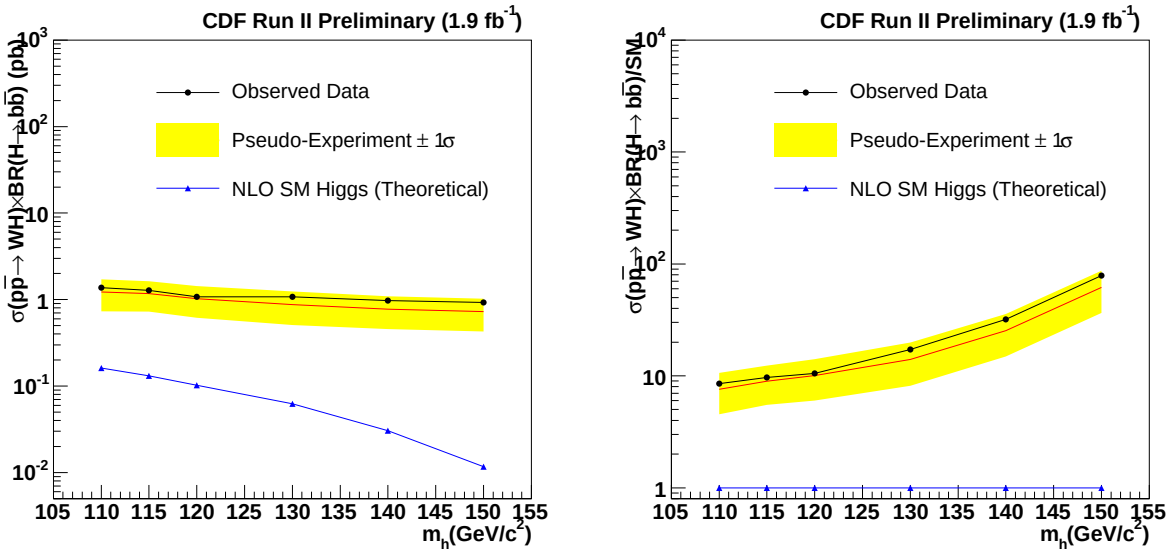

FIG. 7: Observed and predicted rate limits as a function of the Higgs mass hypothesis. Results are for central leptons only. These results are based on the combined two double tag selections and one single tag selection. The plot on the left shows the limits as measured in picobarns. The plot on the right shows the ratio of the limit to the expected SM Higgs cross section.

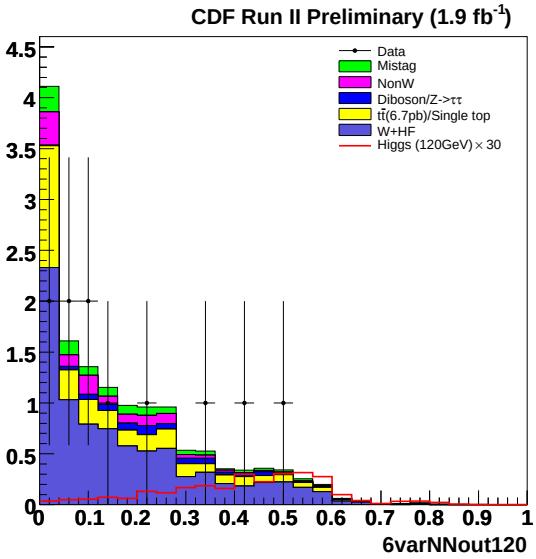

FIG. 8: Neural Network output for double secondary vertex tagged plug electron events.

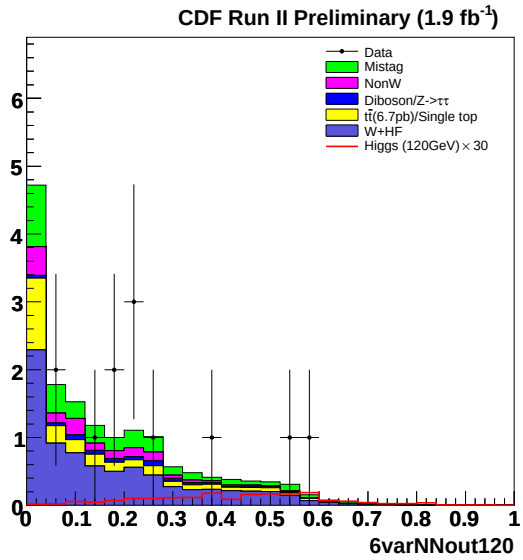

FIG. 9: Neural Network output for one secondary vertex tag and one jet probability tag plug electron events.

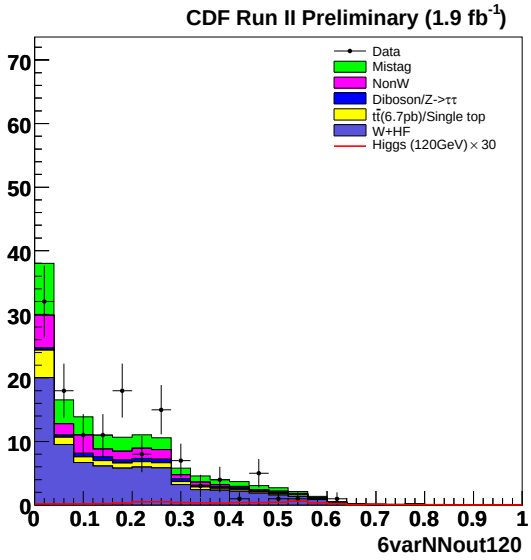

FIG. 10: Neural Network output for one secondary vertex tag with neural network flavor separation plug electron events.

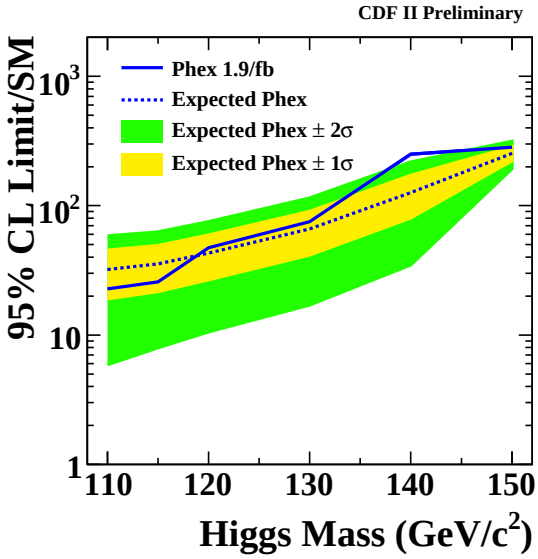

FIG. 11: Observed and predicted rate limits for plug electron events only, shown as a function of the Higgs mass hypothesis. These results are based on the combined two double tag selections and one single tag selection. The plot shows the ratio of the limit to the expected SM Higgs cross section.

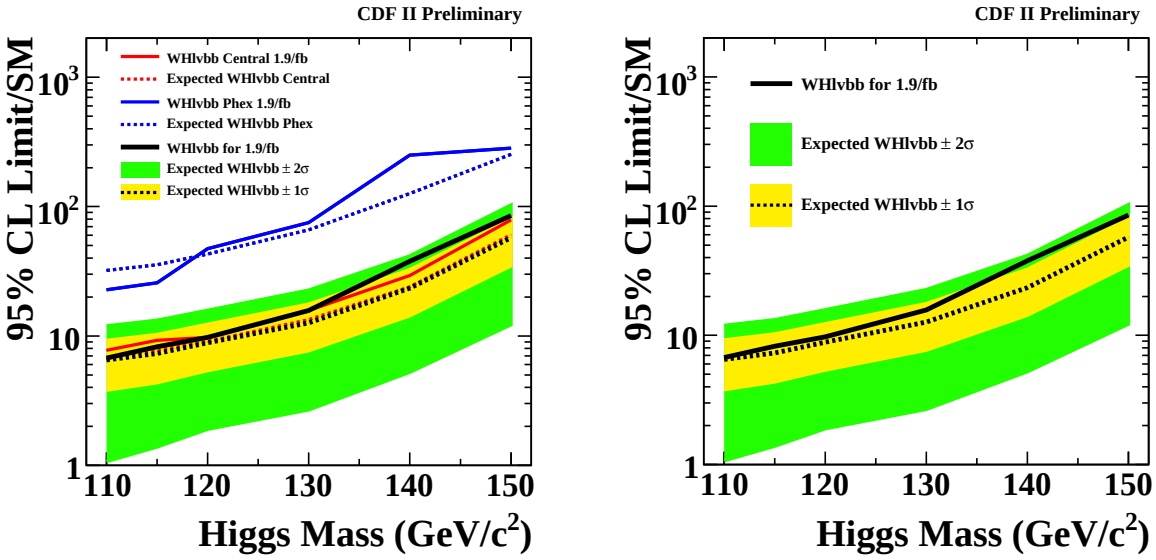

FIG. 12: Observed and predicted rate limits for combined central and plug events, shown as a function of the Higgs mass hypothesis. These results are based on the combined two double tag selections and one single tag selection. The plot shows the ratio of the limit to the expected SM Higgs cross section. The plot on the left shows the observed and expected limits for the plug electrons, the central, and the plug electrons and central combined. The plot on the right shows the observed and expected limits for only the combination of all lepton types.